Silicon isotopes in Antarctic sponges: an interlaboratory comparison

Katharine R. Hendry[1,3,*]

Melanie J. Leng[2]

Laura F. Robinson[1]

Hilary J. Sloane[2]

Jerzy Blusztjan[1]

Rosalind E.M. Rickaby[3]

R. Bastian Georg[3,4]

Alex N. Halliday[3]

1 Department of Marine Chemistry and Geochemistry, Woods Hole Oceanographic Institution, Woods Hole, MA 02543, USA. * Corresponding e-mail address: khendry@whoi.edu.

2 NERC Isotope Geosciences Laboratory, British Geological Survey, Keyworth, Nottingham, NG12 5GG, UK.

3 Department of Earth Sciences, University of Oxford, Parks Road, Oxford, OX1 3PR, UK.

4 Trent University, Worsfold Water Quality Centre, Peterborough, Ontario, Canada.

Abstract

Cycling of deep-water silicon (Si) within the Southern Ocean, and its transport into other ocean basins, may be an important player in the uptake of atmospheric carbon, and global climate. Recent work has shown that the Si isotope (denoted by $\delta^{29}Si$ or $\delta^{30}Si$) composition of deep-sea sponges reflects the availability of dissolved Si during growth, and is a potential proxy for past deep and intermediate water silicic acid concentrations. As with any geochemical tool, it is essential to ensure analytical precision and accuracy, and consistency between methodologies and laboratories. Analytical bias may exist between laboratories, and sponge material may have matrix effects leading to offsets between samples and standards. Here, we report an interlaboratory evaluation of Si isotopes in Antarctic and subAntarctic sponges. We review independent methods for measuring Si isotopes in sponge spicules. Our results show that separate subsamples of non-homogenised sponges measured by three methods yield isotopic values within analytical error for over 80% of specimens. The relationship between $\delta^{29}Si$ and $\delta^{30}Si$ in sponges is consistent with kinetic fractionation during biomineralisation. Sponge Si isotope analyses show potential as palaeoceaongraphic archives, and we suggest Southern Ocean sponge material would form a useful additional reference standard for future spicule analyses.

Keywords: biogeochemistry, Porifera, nutrient, calibration, silicic acid

1. Introduction

1.1. Silicon isotopes and previous interlaboratory calibrations

The use of silicon (Si) isotopes in geosciences has expanded in the past decade to include cosmochemistry (e.g. Georg et al., 2007), earth surface processes (e.g. Opfergelt et al., 2009), palaeoceanography (e.g. de la Rocha et al., 1998; Brzezinksi et al., 2002; Beucher et al., 2007, 2008), palaeolimnology (Street-Perrott et al. 2008, Leng et al., 2009; Swann et al. 2010) and biological systems, including Si uptake by diatoms (de la Rocha et al., 1997), plants (Opfergelt et al., 2006; Hodson et al. 2008) and sponges (de la Rocha, 2003; Hendry et al., 2009; Hendry et al., 2010; Wille et al., 2010).

Si is present in three stable isotopes: ^{28}Si (92.22%), ^{29}Si (4.68%) and ^{30}Si (3.08%). The fractionation factor during a reaction from A to B, α, is defined by Equation 1:

$$ {}^{x}\alpha = \frac{\left(\frac{{}^{x}Si}{{}^{28}Si}\right)_{A}}{\left(\frac{{}^{x}Si}{{}^{28}Si}\right)_{B}} \quad (1) $$

where x is either of the two minor isotopes, ^{29}Si or ^{30}Si. The per mil (‰) Si isotopic composition is expressed relative to the NIST standard, NBS 28, according to Equation 2:

$$ \delta^{x}Si = \left\{ \frac{\left(\frac{{}^{x}Si}{{}^{28}Si}\right)_{sample}}{\left(\frac{{}^{x}Si}{{}^{28}Si}\right)_{NBS\,28}} - 1 \right\} \times 1000 \quad (2) $$

The relationship between measured $\delta^{29}Si$ and $\delta^{30}Si$ can be used to demonstrate mass dependent fractionation, according to Equation 3:

$$^{29}\alpha = {}^{30}\alpha^{z} \quad (3)$$

where z~0.52 and depends on the ratio of the isotope masses and on whether the fractionation reaction is kinetic or in equilibrium (reviewed by Reynolds et al., 2007).

A previous interlaboratory comparison has been published using three isotopic standards: a rock standard IRMM-018, a "Diatomite" standard, and a highly fractionated SiO_2 material, "Big Batch", originally prepared at the University of California, Santa Barbara (UCSB) by Mark Brzezinksi and Christina de la Rocha (Reynolds et al., 2007). However, IRMM-018 is no longer produced commercially and did not show a good level of reproducibility between research groups, either as a result of isotopic heterogeneity or contamination, so is not a useful reference standard.

1.2. Sponge silicon isotopes and deep-water silicic acid

Reconstructing Southern Ocean intermediate and deep $Si(OH)_4$ through time is essential to our understanding of silica cycling, and its potential impact on the carbon cycle. Firstly, diatom blooms rely on upwelling sources of $Si(OH)_4$ because efficient utilization removes almost all of the Si from surface waters (Ragueneau et al., 2000; Falkowski et al., 2004). Secondly, heat transport by the oceans is influenced strongly by high-latitude deep-water formation processes and meridional distribution of deep-water masses. Ocean circulation and biogeographical variations in algal populations results in enriched $Si(OH)_4$ in

Antarctic Bottom Water (AABW) compared to North Atlantic Deep Water (NADW) (Garcia et al., 2006). This difference allows dissolved Si to be used as a tracer of southern component water masses in the Atlantic over 10^3 to 10^4 year timescales. Thirdly, whole ocean changes in Si cycling over long timescales (>10^4-10^5 years) will be reflected in deep water $Si(OH)_4$ concentrations to a greater extent than surface values, which are likely to be influenced by local processes such as productivity (de la Rocha & Bickle, 2005). The Southern Ocean has been the major sink of opal for the past 2 to 3 million years, and is a key source area for such palaeoceanographic records (Cortese et al., 2004).

The Si isotopic composition of sponges has been recognized as a potential archive of deep-water Si chemistry (de la Rocha, 2003; Hendry et al., 2008, 2010; Wille et al., 2010). Siliceous sponges (Phylum Porifera, Classes Demospongea and Hexactinella) produce needle-like skeletal elements, called spicules, from hydrated amorphous silica. Spicules can be further subdivided into larger megascleres and smaller microscleres (Figure 1a). Uptake of ambient $Si(OH)_4$ occurs via a sodium transporter, which resembles active transporters isolated from other metazoans. The silica deposition occurs about a central organic filament in the axial canal of the filament (Schroeder et al., 2004). Biosilicification is carried out by sclerocyte cells both intra- and extracellularly and is controlled by the enzymes silicatein, which promotes condensation reactions, and silicase, which dissolves silica (Uriz et al., 2003; Foo et al., 2004; Müller et al., 2007). Silicatein is the predominant component of the axial filament and is found on the surface of spicules and in the extra-cellular space, resulting in lamellar growth (Müller et al., 2005). During these reactions,

sponges fractionate Si isotopes with respect to the ambient $Si(OH)_4$, such that spicules have some of the lightest Si isotopic signatures known in natural systems (de la Rocha, 2003).

With the development of Si isotopes in sponges as a geochemical proxy, it is essential to determine analytical precision and accuracy, and ensure there are no systematic differences between methodologies. Here, we present an interlaboratory comparison of the Si isotopic composition of sponges from the Southern Ocean and the Antarctic Peninsula. We review two independent methods for sample preparation, using three different instruments for Si isotope analysis. We show that sponge Si isotope ratios are homogeneous and influenced strongly by environmental parameters. Further work on the sponge Si isotope uptake and systematics would benefit greatly from a suitable interlaboratory reference standard.. Although "Diatomite", which contains non-opal impurities, and "Big Batch" reproduced well ($\delta^{30}Si \sim +1.27$ and $-10.48‰$ respectively), neither standard has an isotope composition or microstructure similar to sponges (Schroeder et al., 2008).

2. Methods

2.1. Sample collection and initial preparation

We collected and analysed modern specimens of sponges from a north-south transect across the Southern Ocean, encompassing a range of $Si(OH)_4$ concentrations (12 to 120 μM) and depths (300 to 2500 m). Sponges were collected aboard the *R/V Nathaniel B. Palmer* from sites in the Drake Passage and Scotia Sea (April-May 2008; Figure 1b). Additional samples were collected from Anvers and Adelaide

Islands off the West Antarctic Peninsula. Spicules were isolated from organic matter by heating three times in concentrated HNO_3 and H_2O_2 (reagent grade), rinsing each time with 18 MΩ Milli-Q water. Detrital lithogenic grains were then physically removed until visual inspection showed the sample to comprise pure sponge spicules. The spicules were then further chemically cleaned by heating in 50% HNO_3 and 10% HCl (in-house Teflon distilled) for two hours, followed by five Milli-Q rinses. Subsamples were analysed by three different laboratories using different methods: stepwise fluorination followed by gas sourced Isotope Ratio Mass Spectrometry (IRMS) at the NERC Isotope Geosciences Laboratory (NIGL; Leng & Sloane, 2008), wet alkaline extraction followed by analysis by *NuPlasma* Multi-Collector Inductively Coupled Plasma Mass Spectrometer (MC-ICP-MS) at Oxford University (Georg et al., 2006; Hendry et al., 2010) and wet alkaline extraction followed by analysis by Neptune MC-ICP-MS (this study; van den Boorn et al., 2006; Wille et al., 2010) at Woods Hole Oceanographic Institution (WHOI).

2.2. Stepwise fluorination/IRMS (NIGL)

The subsamples were processed using stepwise fluorination, designed for both $\delta^{30}Si/\delta^{29}Si$ and $\delta^{18}O$ analysis of silica, to convert the Si (and O) to a gaseous phase (Leng & Sloane, 2008). Firstly, the samples were dehydrated at 250°C to remove surface and loosely bound water. Secondly, the samples went through a pre-fluorination reaction with a stoichiometric deficient quantity of bromine pentafluoride at low temperature to remove hydroxyl groups and any remaining loosely bound water. Thirdly, the samples were fully fluorinated at 450°C for 12 hours, during which the Si is converted to silicon tetrafluoride (SiF_4), which is then measured off-line for ^{28}Si, ^{29}Si and ^{30}Si simultaneously using a Finnegan MAT253 IRMS. Repeat

154 measurements of standards indicate a reproducibility of <0.24‰ (2SD) for $\delta^{29}Si$ and
155 $\delta^{30}Si$.

156 *2.3. Wet alkaline extraction/NuPlasma MC-ICP-MS (Oxford)*

157 The subsamples were dissolved by wet alkaline extraction (Cardinal et al.,
158 2007). Briefly, the spicules were dissolved in 4ml 0.2M NaOH per mg silica, left
159 at 100°C for three days, and sonicated on a daily basis to aid dissolution. The
160 solutions were acidified with 0.2M HCl (in-house Teflon distilled) to a pH > 2.

161 The Si concentrations of the dissolved samples and standards were determined
162 using a heteropoly blue photospectrometric method (Ultra Low Range solutions,
163 Hach). Quantitative separation of Si from major ions was achieved using a cation
164 exchange resin (BioRad AG50W-X12; Georg et al., 2006). The standard and
165 samples (<0.4 ml) were introduced to the column, which contained a volume of
166 wet resin at neutral pH suitable for the amount of Na added (0.8 to 1.8 ml).
167 $Si(OH)_4$ is in equilibrium with the anionic silicate species $H_3SiO_4^-$ for the pH
168 range 2-8 (Georg et al., 2006), and can simply be eluted with Milli-Q water.
169 Recent studies have shown pH does not affect Si yield or fractionation on the
170 column (Savage et al., 2010). Our previous tests have shown this method results
171 in 100% yields for both commercially available Si solutions and dissolved
172 biogenic opal samples (Hendry et al., 2010; Hendry, unpublished data). There
173 are traces of organic matter bound within biogenic opal, including sponge
174 spicules, which may form small silico-organic complexes that cannot be removed
175 from the Si and may cause instabilities with plasma source mass spectrometry.
176 However, our measurements of the organic content of sponge spicules show the

177 organic content is ~ 0.1% or lower, and any problems arising from this material
178 will be minimal.

179 The Si isotope measurements of the Si isotopes (^{28}Si, ^{29}Si and ^{30}Si) use the
180 *NuPlasma* MC-ICP-MS (University of Oxford), again allowing simultaneous
181 measurement of the different isotopes. The mass spectrometer was operated in
182 medium resolution mode to resolve interferences on masses 28 (e.g. $^{14}N^{14}N^{+}$,
183 $^{12}C^{16}O^{+}$), 29 ($^{14}N^{15}N^{+}$, $^{13}C^{16}O^{+}$, $^{12}C^{17}O^{+}$) and 30 ($^{15}N^{15}N^{+}$, $^{13}C^{17}O^{+}$, $^{12}C^{18}O^{+}$).
184 Samples were introduced via a self-aspirating PFA micro concentric nebuliser
185 (ESI) plugged into a Cetac ARIDUS-2 desolvator unit, supplied only with Ar and
186 not N_2. Uptake rates varied slightly, but were typically around 100 µL min^{-1}
187 (Table 1). The samples were bracketed with a concentration-matched NBS28
188 standard (~600 ppb Si) to correct for mass bias and drift (Georg et al., 2006;
189 Reynolds et al., 2007), and isotope ratios calculated according to equation 2.
190 Standards were analysed before every batch run to ensure accuracy. Repeat
191 dissolutions and repeat aliquots of the same dissolution indicate a good level of
192 reproducibility around 0.1‰ (2SD) for $\delta^{30}Si$ and 0.2‰ (2SD) for $\delta^{30}Si$ (Hendry
193 et al., 2010). Full details of experimental set-up and quality control criteria are
194 published elsewhere (Georg et al., 2007; Savage et al., 2010).

195 *2.4. Wet alkaline extraction/Neptune MC-ICP-MS (WHOI)*

196 Aliquots of a solution prepared from a sponge collected from Anvers Island off
197 the West Antarctic Peninsula (LMG08), prepared by wet alkaline extraction and
198 column separation as outlined above, were introduced into the Thermo Neptune
199 MC-ICP-MS instrument. The instrument was operated in a dry plasma mode,
200 with the sample introduced via a self-aspirating PFA micro concentric nebuliser,

plugged into an ARIDUS-1 (not connected to N_2) with an uptake rate of 50 µL min^{-1}., in high-resolution mode to resolve potential interferences as outlined above. The instrument was left to stabilize after plasma ignition for approximately an hour before tuning on a daily basis, during which gas flow and ion optics are optimized for maximum sensitivity and peak shape on ^{28}Si (Figure 2). Peak centering was carried out on ^{28}Si prior to measurement. Operating conditions are outlined in Table 1.

Mass bias and drift were accounted for by standard-sample bracketing matching samples and bracketing standards. Our initial tests showed intensity matching of bracketing standards and samples of within 20% resulted in acceptable levels of reproducibility for the known reference standards (± 0.15‰ for $\delta^{30}Si$). To provide a conservative limit, the bracketing standards and samples were intensity matched within 15%. The blank is monitored by analyzing a 0.05N HCl solution run prior to and after each standard-sample bracket, and is <1% of the signal (Table 1). Blank corrections do not make significant differences to the calculated $\delta^{29}Si$ or $\delta^{30}Si$ for standards or samples.

Values of $\delta^{29}Si$ and $\delta^{30}Si$ were calculated offline using Equation 2, taking an average of the two bracketing standards for each sample. Data that did not meet strict quality control criteria were rejected, meeting guidelines based on van den Boorn et al. (2006):

a) Initial tests showed that for a standard deviation of greater than 1 x 10^{-5} on either ^{29}Si /^{28}Si or ^{30}Si /^{28}Si ratios resulted in an error greater than ~ 0.2‰ on the resulting $\delta^{29}Si$ and $\delta^{30}Si$ values, which were generally non-mass dependent.

Any samples or bracketing standards run with a standard deviation above this threshold were rejected.

b) If the difference between two successive bracketing standards exceeded 0.4‰ for $\delta^{30}Si$ (double the approximate long-term reproducibility 2SD), the data were rejected.

The mean of all replicates that meet the criteria above (typically n = 3) for each aliquot was calculated and reported relative to NBS28.

Measurement precision was assessed using previously calibrated standards ("Diatomite" and "Big Batch"; Reynolds et al., 2007). Diatomite showed a good level of reproducibility, with $\delta^{29}Si \sim 0.66$‰ and $\delta^{30}Si \sim 1.26$‰ depending on whether all measurements are included, or mean values of each aliquot undergoing independent chemical separation (Table 2). Big Batch showed greater variability (Table 2), appearing to be more sensitive to drift due to larger fractionation, perhaps as a result of matrix effects from its high molybdenum content (Reynolds et al., 2007). Repeat measurements of sample aliquots, within and between runs, show typical variability <0.1‰ for $\delta^{29}Si$ and $\delta^{30}Si$. However, the sample size of measurements for each aliquot is small (n~3), such that calculating standard deviations is not valid, and so the long-term reproducibility for diatomite is used as a more conservative estimate of total error (Table 2).

All three methods show a very similar long-term reproducibility (2SD ~ 0.2‰ for $\delta^{30}Si$), in agreement with the finding of the previous interlaboratory

calibration of standards that differences between reported results should be limited to 0.2‰ for $\delta^{30}Si$ (Reynolds et al., 2007).

3. Results

The $\delta^{30}Si$ values of sixteen modern sponges measured at NIGL varied from approximately –0.5 to –4‰ (Table 3), all in range of other published values (de la Rocha, 2003; Hendry et al., 2010; Wille et al., 2010). Subsamples from these specimens had been previously analysed at Oxford (previously reported in Hendry et al., 2010). Note that although the spicules were not homogenized prior to analysis, subsample measurements of any particular specimen are in good agreement (Figure 3; regressing Oxford data on NIGL data yields r=0.97, slope = 1.09, intercept = 0.06‰). Over 80% of the specimens yielded $\delta^{30}Si$ values that agreed within ±0.2‰, (i.e. agreement within analytical error), and all agreed within ±0.3‰ (including OT3-111 and DR-111, two specimens of the same species of demosponge). Repeat subsamples analysed at NIGL agreed within ±0.1‰ for $\delta^{30}Si$ (Table 3).

Subsamples from a sponge collected near the Antarctic Peninsula, LMG08, were measured by Oxford (Hendry et al,. 2010), NIGL and WHOI (both this study), and also showed a high level of reproducibility (Figure 4; Oxford $\delta^{30}Si$ = –3.36 ±0.16‰ (one aliquot with repeat measurements; n=8), NIGL (one aliquot) $\delta^{30}Si$ = –3.3‰, WHOI (all measurements, n = 16) = –3.41 ±0.18‰; WHOI (mean values for independent aliquots, n = 4) $\delta^{30}Si$ = –3.40 ±0.10‰, for 2SD).

All three laboratories show mass dependent measurements for sponge samples, with the slope of the three isotope plot of $\delta^{29}Si$ vs. $\delta^{30}Si \sim 0.51$ (Figure 5, Table 4, see discussion below).

4. Discussion

4.1. Isotopic homogeneity in sponges

The agreement between the different laboratories, utilising different preparation and measurement techniques, indicates that $\delta^{30}Si$ measurements obtained for Southern Ocean sponges are robust and there is no method dependent fractionation of Si isotopes. Furthermore, given that the subsamples were not taken from a homogenized mass of spicules, our data also indicate there is a high level of homogeneity within Southern Ocean sponges. There are other lines of evidence for isotopic homogeneity within specimens of Southern Ocean sponge:

a) Dermal and perenchymal spicules in sponge NBP0805 TB4-24

Spicules taken from external layers (dermal) and internal layers (perenchymal) from a sponge collected in the Drake Passage have, within error, the same isotopic composition (dermal $\delta^{30}Si = -2.87‰$ and perenchymal $\delta^{30}Si = -2.96‰$; Hendry et al., 2010).

b) Core top megaspicules and modern sponge mixed spicules

Core top measurements of megaspciules picked from Scotia Sea sediments ($\delta^{30}Si \sim -3.9‰$) are within error of modern sponges living near to the core site ($\delta^{30}Si$

290 ~ –4.1‰; Hendry et al., 2010), comprising both mega and microspicules (Figure
291 1a).

292 *4.2. Kinetic uptake of Si by sponges*

293 The relationship between ambient $Si(OH)_4$ and isotopic composition of sponges
294 suggests a growth rate effect (Hendry et al., 2010). Kinetic uptake of Si has been
295 observed during sponge growth (Frølich & Barthel, 1997) and supported by the
296 highly fractionated nature of sponge Si isotopes, and by theoretical isotopic
297 fractionation models (Wille et al., 2010). The relationship between $\delta^{29}Si$ and
298 $\delta^{30}Si$ can be used to determine whether kinetic or equilibrium fractionation has
299 occurred: equilibrium fractionation yields a slope on a three-isotope plot (Figure
300 5) of 0.518 whereas kinetic fractionation results in a slopes of either 0.509 or
301 0.505 for Si atoms and SiO_2 respectively (Reynolds et al., 2007). Data from all
302 three laboratories are consistent with kinetic fractionation (either Si or SiO_2,
303 Reynolds et al., 2007) within 95% confidence intervals calculated by model II
304 linear regressions (Table 4), whereas only data from one laboratory is within
305 range of equilibrium fractionation. This supports the notion of kinetic uptake of
306 Si by deep-sea sponges in the Southern Ocean.

307 *4.3. Use of sponge spicules as geochemical archives*

308 Understanding the impact of surface biological production on carbon export in
309 the past relies on the reconstruction of the nutrient supply from upwelling deep-
310 waters, both within the Southern Ocean and further afield. Sponges are an ideal
311 marine geochemical archive of deep-water nutrients, given their ubiquitous
312 distribution on the oceans. We confirm that Antarctic sponge Si isotopic

313 composition show a robust relationship with ambient $Si(OH)_4$, are internally
314 homogeneous, and measurements are reproducible irrespective of preparation
315 and analytical method. Two independent calibrations, produced by different
316 laboratories, show ambient $Si(OH)_4$ is the dominant control over both the Si
317 isotopic composition of, and fractionation by, sponges collected in different
318 sectors of the Southern Ocean (Hendry et al., 2010; Wille et al., 2010; Figure 1b,
319 6). There is no consistent species specific offset in isotopic composition or
320 fractionation: different species from the same site show similar isotopic
321 composition and two specimens of the same species from different $Si(OH)_4$
322 environments show different isotopic compositions (Hendry et al., 2010). There
323 is no evidence for a significant influence of temperature, pH, or salinity on
324 isotopic fractionation (Hendry et al., 2010; Wille et al., 2010). The scatter in the
325 $Si(OH)_4$-$\delta^{30}Si$ calibration, which may reflect secondary vital effects, results in an
326 uncertainty of any reconstructing Si(OH)4 concentration of approximately ± 20
327 μM (Hendry et al., 2010).

328 The relationship between $Si(OH)_4$ and $\delta^{30}Si$ from the two calibrations agree well
329 between $Si(OH)_4$ concentrations of ~ 5 and 80 μM. However, at concentrations
330 ~ 2 μM, only sampled by one calibration, sponge $\delta^{30}Si$ become isotopically
331 heavier than expected, suggesting either an exponential relationship with
332 $Si(OH)_4$ concentration (Wille et al., 2010) or a non-linearity arising from
333 physiological stress under low Si. Given the scatter in the calibration, a simple
334 linear fit between $\delta^{30}Si$ and $Si(OH)_4$ is likely adequate for most applications; for
335 shallow water environments experiencing low $Si(OH)_4$, an exponential fit may be
336 appropriate. Further work is required to validate this calibration in other ocean

basins, experiencing different nutrient regimes and physical environmental parameters. Culturing studies growing sponges under extreme concentrations of $Si(OH)_4$ (less than 5 μM and greater than 120 μM) may also elucidate the linear vs. exponential nature of the relationship between $Si(OH)_4$ and $\delta^{30}Si$, and resolve the cause of scatter in the calibrations.

4.4. Sponge $\delta^{29}Si$ and $\delta^{30}Si$ standard

The isotopic homogeneity in sponges makes them an ideal target for a reference standard, which would be particularly valuable should sponge spicules become a more commonly used geochemical archive. The sponge LMG08 has now been analysed by three laboratories, using two different preparation methods and three different instruments, and yielded (within error) the same value (mean $\delta^{29}Si$ value from the three laboratories = –1.72 ± 0.01‰, mean $\delta^{29}Si$ value of all measurements = –1.72‰, 2SD = 0.08‰; mean $\delta^{30}Si$ value from the three independent laboratories = –3.35 ± 0.06‰, mean $\delta^{30}Si$ value of all measurements = –3.37‰, 2SD = 0.17‰; Figure 4). Additional subsamples are available from the authors for future interlaboratory tests.

5. Conclusion

The Southern Ocean is an important location for studying deep-water Si cycling because of the regional importance of global biological productivity and its sensitivity to well documented proximal climatic changes. Sponge spicule $\delta^{29}Si$ and $\delta^{30}Si$ are promising new proxies for past deep-water silicic acid concentrations, and Southern Ocean downcore records of spicules could be applied to a wide range of climatic and palaeoceanographic questions. We show

here that Si isotopic measurements of Antarctic sponge spicules are robust and reproducible, confirming that the overriding control over silicon isotopes is the ambient $Si(OH)_4$ concentrations in which the sponges grow. The relationship between $\delta^{29}Si$ and $\delta^{30}Si$ is consistent with kinetic fractionation during sponge growth. Lastly, we suggest Southern Ocean sponges would act as an ideal new standard for future spicule analyses.

Acknowledgements

The authors would like to thank the captain and crew of the *R/V Nathaniel B. Palmer* (cruise NBP0805; Program Manager Thomas Wagner). Thanks also to Rhian Waller (University of Hawaii), Laura Schejter (INIDEP, Argentina), Jade Berman (University of Victoria, Wellington) and Andy Clarke (British Antarctic Survey) for sponge samples and help with identification. Thanks to Maureen Auro and Scot Birdwhistell (WHOI) for assistance in the laboratory, and Tim Eglinton, Daniel Montlucon and Carl Johnson for analysis of spicule organic matter content. Thanks to David Walton, Michael Ellwood, Martin Wille and an anonymous reviewer for constructive comments on the manuscript. Cruise NBP0805 was funded by NSF Office of Polar Programs (OPP) Antarctic Sciences (grant number ANT-0636787). KH is funded by a Doherty Postdoctoral Scholarship at WHOI, and the work has also been funded by the Natural Environment Research Council (NERC) grant NE/F005296/1 and an Antarctic Science Bursary. The authors declare no competing financial interests.

References

Beucher, C.P., Brzezinksi, M.A., Crosta, X., 2007. Silicic acid dynamics in the glacial sub-Antarctic: Implications for the silicic acid leakage hypothesis. Global Biogeochemical Cycles. 21, doi:10.1029/2006GB002746.

Beucher, C.P., Brzezinksi, M.A., Jones, J.L., 2008. Sources and biological fractionation of silicon isotopes in the Eastern Equatorial Pacific. Geochimica et Cosmochimica Acta. 72, 3063-3073.

Brzezinski, M.A., Sigman, D.M., Sarmiento, J.L., Matsumoto, K., Gruber, N., Rau, G.H., Coale, K.H., 2002. A switch from $Si(OH)_4$ to NO_3^- depletion in the glacial Southern Ocean. Geophysical Research Letters. 29, 1564.

Cardinal, D., Savoye, N., Trull, T.W., Dehairs, F., E.E., K., Fripiat, F., Tison, J.-L., André, L., 2007. Silicon isotope in spring Southern Ocean diatoms: large zonal changes despite homogeneity among size fractions. Marine Chemistry. 106, 46-62.

Cortese, G., Gersonde, R., Hillendbrand, C.-D., Kuhn, G., 2004. Opal sedimentation shifts in the World Ocean over the last 15 Myr. Earth and Planetary Science Letters. 224, 509-527.

de la Rocha, C., Brzezinksi, M.A., DeNiro, M.J., 1997. Fractionation of silicon isotopes by marine diatoms during biogenic silica formation. Geochimica Cosmochimica Acta 61, 5051-5056.

de la Rocha, C., Brzezinksi, M.A., DeNiro, M.J., Shemesh, A., 1998. Silicon isotope composition of diatoms as an indicator of past oceanic change. Nature. 395, 680-683.

de la Rocha, C.L., 2003. Silicon isotope fractionation by marine sponges and the reconstruction of the silicon isotope composition of ancient deep water. Geology. 31, 423-426.

de la Rocha, C., Bickle, M., 2005. Sensitivity of silicon isotopes to whole-ocean changes in the silica cycle. Marine Geology. 217, 267-282.

Falkowski, P.G., Katz, M.E., Knoll, A.H., Quigg, A., Raven, J.A., Schofield, O., Taylor, F.J.R., 2004. The evolution of modern eukaryotic phytoplankton. Science. 305, 354-360.

Foo, C.W.P., Huang, J., Kaplan, D.L., 2004. Lessons from seashells: silica mineralization via protein templating. Trends in Biotechnology. 22, 577-585.

Frøhlich, H., Barthel, D., 1997. Silica uptake of the marine sponge Halichondria panicea in Kiel Bight. Marine Biology. 128, 115-125.

Garcia, H.E., R.A. Locarnini, T.P. Boyer, and J.I. Antonov. World Ocean Atlas 2005, volume 4: Nutrients (phosphate, nitrate, silicate). S.Levitus, Ed. NOAA Atlas NESDIS 64, U.S. Government Printing Office, Washington, D.C., 396pp (2006).

Georg, R.B., Halliday, A.N., Schauble, E.A., Reynolds, B.C., 2007. Silicon in the Earth's core. Nature. 447, 1103-1106.

Georg, R.B., Reynolds, B.C., Frank, M., Halliday, A.N., 2006. New sample preparation techniques for the determination of Si isotopic composition using MC-ICPMS. Chemical Geology. 235, 95-104.

Hendry, K.R., Georg, R.B., Rickaby, R.E.M., Robinson, L.F. & Halliday, A.N. (2009) Sponge Spicules as Recorders of Deep-Water Silicic Acid. *Geochim. Cosmochim. Acta*, 73, A522.

Hendry, K.R., Georg, R.B., Rickaby, R.E.M., Robinson, L.F. & Halliday, A.N., 2010. Deep ocean nutrients during the Last Glacial Maximum deduced from sponge spicule silicon isotopes. Earth and Planetary Science Letters, doi:10.1016/j.epsl.2010.02.005.

Hodson, M.J., Parker, A.G., Leng, M.J., Sloane, H.J., 2008. Silicon, oxygen and carbon isotpes in wheat (*Triticum aestivum* L.) phytoliths - implications for palaeoecology and archaeology. Journal of Quaternary Science. 23.

Leng, M.J., Sloane, H.J., 2008. Combined oxygen and silicon isotope analysis of biogenic silica. Journal of Quaternary Science. 23, 313-319.

Leng, M.J., Swann, G.E.A., Hodson, M.J., Tyler, J.J., Patwardhan, S.V., Sloane, H.J., 2009. The potential use of silicon isotope composition of biogenic silica as a proxy for environmental change. SILICON. 1, 65-77.

Müller, W.E.G., Schloßmacher, U., Wang, X., Boreiko, A., Brandt, D., Wolf, S.E., Tremel, W., Schroeder, H.C., 2007. Poly(silicate)-metabolizing silicatein in siliceous spicules and silicasomes of demosponges comprises dual enymatic activities (silica polymerase and silica esterase). FEBS Journal. 275, 362-370.

Opfergelt, S., Cardinal, D., Henriet, C., Andre, L., Delvaux, B., 2006. Silicon isotope fractionation bewteen plant parts in banana: in situ vs. in vitro. Journal of Geochemical Exploration. 88, 224-227.

Opfergelt, S., de Bournonville, G., Cardinal, D., Andre, L., Delstanche, S., Delvaux, B., 2009. Impact of soil weathering degree on silicon isotopic fracitonation during adsorption onto iron oxides in basaltic ash soils, Cameroon. Geochimica et Cosmochimica Acta. 73, 7226-7240.

Ragueneau, O., Tréguer, P., Leynaert, A., Anderson, R.F., Brzezinksi, M.A., DeMaster, D.J., Dugdale, R.C., Dymond, J., Fischer, G., Francois, R., Heinze, C., Maier-Raimer, E., Martin-Jezequel, V., Nelson, D.M., Quéguiner, B., 2000. A review of the Si cycle in the modern ocean: recent progress and missing gaps in the application of biogenic opal as a paleoproductivity proxy. Global and Planetary Change. 26, 317-365.

Reynolds, B.C., Aggarwal, J., Andre, L., Baxter, D., Beucher, C., Brzezinksi, M.A., Engstrom, E., Georg, R.B., Land, M., Leng, M.J., Opfergelt, S., Rodushkin, I., Sloane, H.J., van der Boorn, S.H.J.M., Vroon, P.Z., Cardinal, D., 2007. An inter-laboratory comparison of Si isotope reference materials. Journal of Analytical Atomic Spectrometry. 22, 561-568.

Savage, P.S., Georg, R.B., Armytage, R.M.G., Williams, H.M., Halliday, A.N., 2010. Silicon isotope homogeneity in the mantle. Earth and Planetary Science Letters.

Schroeder, H.C., Wang, X., Tremel, W., Ushijima, H., Müller, W.E.G., 2008. Biofabrication of biosilica-glass by living organisms. Natural Products Reports.

25, 433-636.

Street-Perrott, F.A., Barker, P.A., Leng, M.J., Sloane, H.J., Wooller, M.J., Ficken, K.J., Swain, D.L., 2008. Towards an understanding of Late Quaternay variations in the continental biogeochemical cyle of silicon: multi-isotope and sediment-flux data for Lake Rutundu, Mt. Keyna, East Africa, since 38ka BP. Journal of Quaternary Science. 23, 375-387.

Swann, G.E.A., Leng, M.J., Juschus, O., Melles, M., Brigham-Grette, J., Sloane, H.J., 2010. A combined oxygen and silicon diatom isotope record of Late Quaternary cnge in Lake El'gygytgyn, North East Siberia. Quaternary Science Reviews. 29, 774-789.

Uriz, M.J., Turon, X., Becerro, M.A., 2000. Silica deposition in Demosponges: spiculogenesis. Cell and Tissue Research. 301, 299-309.

Uriz, M.J., Turon, X., Becerro, M.A., Agell, G., 2003. Siliceous spicules and skeleton frameworks in sponges: origin, diversity, ultrastructural patterns, and biological functions. Microscopy Research and Technique. 62, 279-299.

van den Boorn, S.H.J.M., Vroon, P.Z., van Belle, C.C., van der Wagt, B., Schwieters, J., van Bergen, M.J., 2006. Determination of silicon isotope ratios in silicate minerals by high-resolution MC-ICP-MS using a sedium hydroxide sample digestion method. Journal of Analytical Atomic Spectrometry. 21, 734-742.

Wille, M., Sutton, J., Ellwood, M.J., Sambridge, M., Maher, W., Eggins, S., Kelly, M., 2010. Silicon isotopic fractionation in marine sponges: a new model for understanding silicon isotopic fractionation in sponges. Earth and Planetary Science Letters. doi:10.1016/j.epsl.2010.1001.1036.

Figure 1a: Scanning electron micrographs of sponge spicules: i) *Acoelocalyx* sp. and ii) *Rosella* sp.

Figure 1b: Map of sample collection area. Black triangles show location of modern sponges from the Scotia sea/Drake Passage (Hendry et al., 2010; this study) and the Pacific Sector (Wille et al., 2010). The cross shows the location off Anvers Island of sponge LMG08, analysed by Hendry et al. (2010) and NIGL/WHOI (this study). Map produced by K. Scanlon, USGS.

Figure 2: Peak scans for silicon isotopes ^{28}Si (black), ^{29}Si (dark grey) and ^{30}Si (pale rey) in high-resolution and dry plasma mode, obtained with a 1.5 ppm solution of Si in ~ 0.05N Teflon-distilled HCl. Note the vertical exaggeration for ^{29}Si (x 13.88) and ^{30}Si (x 16.35). The measurements were carried out on the left side of the peak plateau to avoid the interferences, clearly visible in high-resolution mode (the black arrow shows the position of the magnet).

Figure 3: Interlaboratory comparison of sponge silicon isotopes, measured by *NuPlasma* MC-ICP-MS at Oxford (Hendry et al., 2010) and Finnegan MAT253 at NIGL (this study). Error bars show long-term reproducibility (2SD). Note that measurements were made on non-homogenised subsamples of sponge specimens, explaining the small variations between laboratories. The grey diamond shows sponge LMG08. Solid line shows 1:1, dashed lines show ±0.2‰.

Figure 4: Repeat measurements of different subsamples of sponge LMG08, collected near Anvers Island off the West Antarctic Peninsula. Different aliquots of a subsample were measured at WHOI on different occasions over four months. 1) All measurements made at WHOI (error bars show 2SD); 2) the mean value for each aliquot measured at WHOI (error bars show 2SD); 3) subsample measure at NIGL (error bars show long-term reproducibility 2SD); 4) mean value for the subsample measured in Oxford (mean of 8 repeat measurements, error bars show 2SD). The grey hatched area shows the mean value for all measurements (±0.2‰).

Figure 5: Three-isotope plot of all the silicon isotope measurements of all sponge samples analysed at the three laboratories. The slope of the plot is consistent with mass dependent fractionation, such that $\delta^{29}Si \sim 0.51\ \delta^{30}Si$. Error bars show long-term reproducibility (2SD). The line shows mass dependent fractionation with slope 0.51.

Figure 6: Two independent studies of Southern Ocean sponge silicon isotopes from the Drake Passage/Scotia Sea (Figure 1b; Hendry et al., 2010) and the Pacific Sector (Wille et al., 2010). A) The relationship between the sponge silicon isotope composition and ambient silicic acid; B) the relationship between the fractionation factor, $\Delta\delta^{30}Si$, defined as the difference between the isotopic composition of the sponge and ambient seawater:

$$\Delta\delta^{30}Si \approx \delta^{30}Si_{sponge} - \delta^{30}Si_{seawater}$$

561

Parameter	Operating conditions and comments	
	Neptune (High resolution)	NuPlasma (Medium resolution)
Cones	Nickel X-cones	Nu instrument experimental WA cones
Nebulizer uptake rate	50 μL per minute	100 μL per minute
Cup configuration	Centre cup – left "shoulder" of ^{28}Si	L5 - ^{28}Si
	H1 – ^{29}Si	Ax – ^{29}Si
	H2 – ^{30}Si	H6 – ^{30}Si
Cycles/block	30	20
Integration time/cycle	4.2 seconds	8 seconds
Sensitivity	10-15V for 1.5 ppm Si (^{28}Si)	~10V for 0.6 ppm Si (^{28}Si)
	300-600 mV for 1.5 ppm Si (^{29}Si & ^{30}Si)	300-500 mV for 0.6 ppm Si (^{29}Si & ^{30}Si)
Blank	~ 50 mV on ^{28}Si	~30 mV on ^{28}Si
Blank/Signal	<1% (typically ~0.5-0.8%)	<1% (typically <0.5%)

562 Table 1: Operating conditions of the Neptune MC-ICP-MS at WHOI. Note that the
563 senstitivies reported are for high resolution settings on the Neptune, and
564 medium resolution settings on the NuPlasma.

Standard	$\delta^{30}Si$ (‰)	$\delta^{30}Si$ (‰) WHOI	
	(Reynolds et al., 2007)	All measurements	Mean values for each aliquot
Diatomite	+1.26 (0.22)	+1.25 (0.12) n=15	+1.28 (0.07) n=5
Big Batch	–10.48 (0.22)	–10.61 (0.14) n=9	–10.61 (0.15) n=3

565 Table 2: $\delta^{30}Si$ measurements of standards, comparing a previous interlaboratory
566 comparison (Reynolds et al., 2007), and measurements made at WHOI (this
567 study). Numbers in parentheses show 1SD.

568

569

570

Specimen Code	$\delta^{29}Si$ (‰)	$\delta^{30}Si$ (‰)
NBP0805-TB1-3	–0.56	–1.05
NBP0805-TO1-57	–1.69	–3.27
	–1.68	–3.28
NBP0805-TB4-24	–1.21	–2.36
NBP0805-DR29-47	–1.80	–3.63
NBP0805-TO1-27	–1.91	–3.71
NBP0805-DR7-47	–1.69	–3.29
NBP0805-TB4-3	–0.87	–1.72
NBP0805-DR34-47	–1.15	–2.22
NBP0805-DR35-111	–1.23	–2.39
NBP0805-TB1-6	–0.54	–1.02
	–0.48	–0.90
NBP0805-DR13-47	–1.55	–3.00
NBP0805-TO3-111	–1.36	–2.62
	–1.26	–2.43
NBP0805-TO3-100	–1.55	–2.99
	–1.49	–2.94

NBP0805-TB4-27	–1.34	–2.59
NBP0805-DR16-27	–2.04	–3.94
LMG08	–1.71	–3.29

571 Table 3: Sponge silicon isotopes measured by IRMS at NIGL. For more
572 information about the specimens, see Hendry et al., 2010.

Laboratory	Gradient $\delta^{29}Si$ vs. $\delta^{30}Si$			Intercept $\delta^{29}Si$ vs. $\delta^{30}Si$		
		Max	Min		Max	Min
Oxford	0.504	0.516	0.492	–0.021	+0.016	–0.057
NIGL	0.507	0.519	0.500	–0.021	+0.012	–0.054
WHOI	0.509	0.515	0.502	–0.007	+0.014	–0.027

573 Table 4: A comparison of the linear regressions of $\delta^{29}Si$ on $\delta^{30}Si$ at the three
574 laboratories (model II linear regression, calculated using R, showing 95%
575 confidence intervals). Note that all laboratories show results consistent with
576 kinetic fractionation (gradient = 0.505 or 0.509); only one laboratory shows
577 results consistent also with equilibrium fractionation (gradient = 0.518).

578

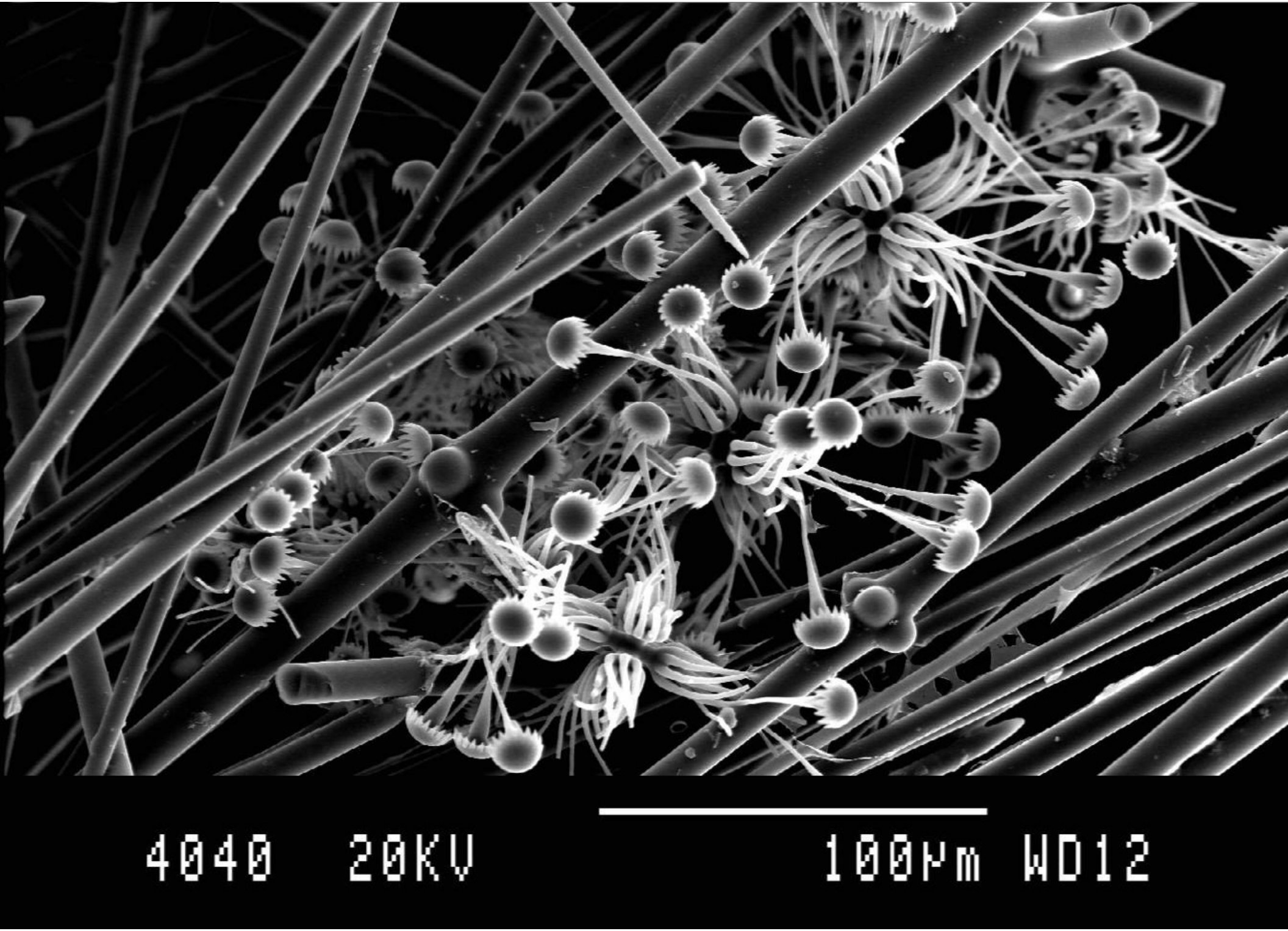
4040 20KV
100µm WD12

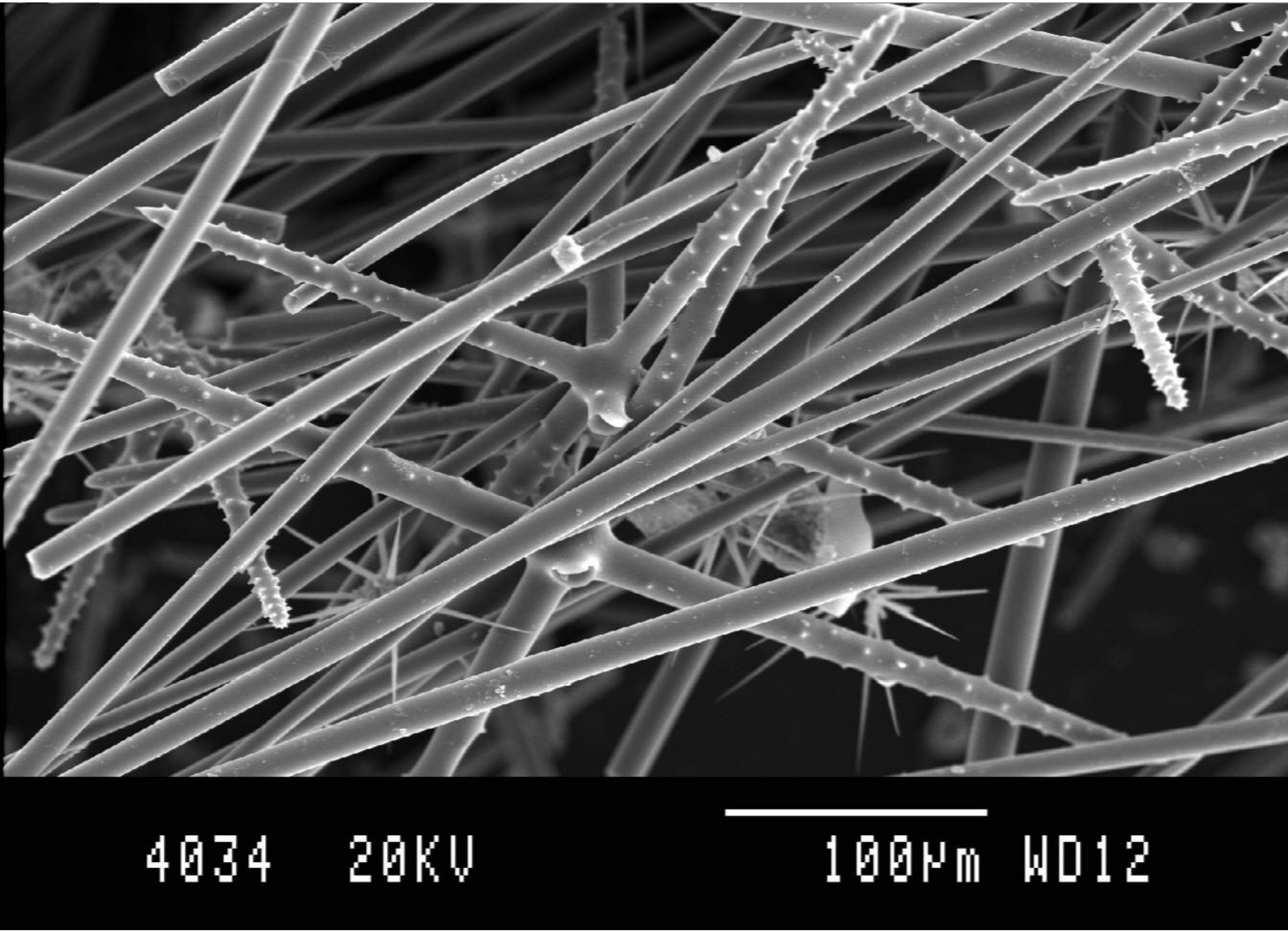
4034 20KV
100μm WD12

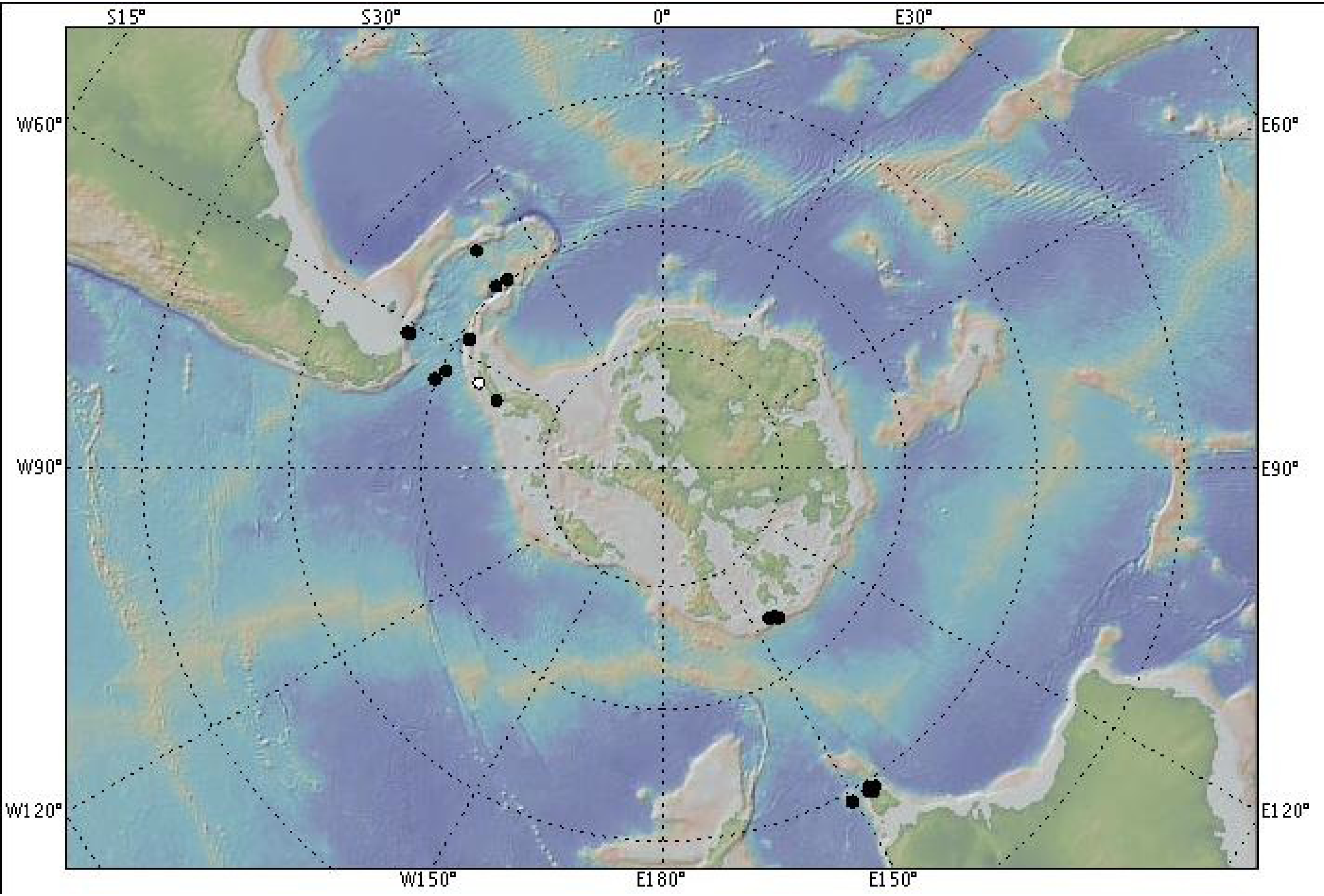
S15°
S30°
0°
E30°
W60°
E60°
W90°
E90°
W120°
E120°
W150°
E180°
E150°

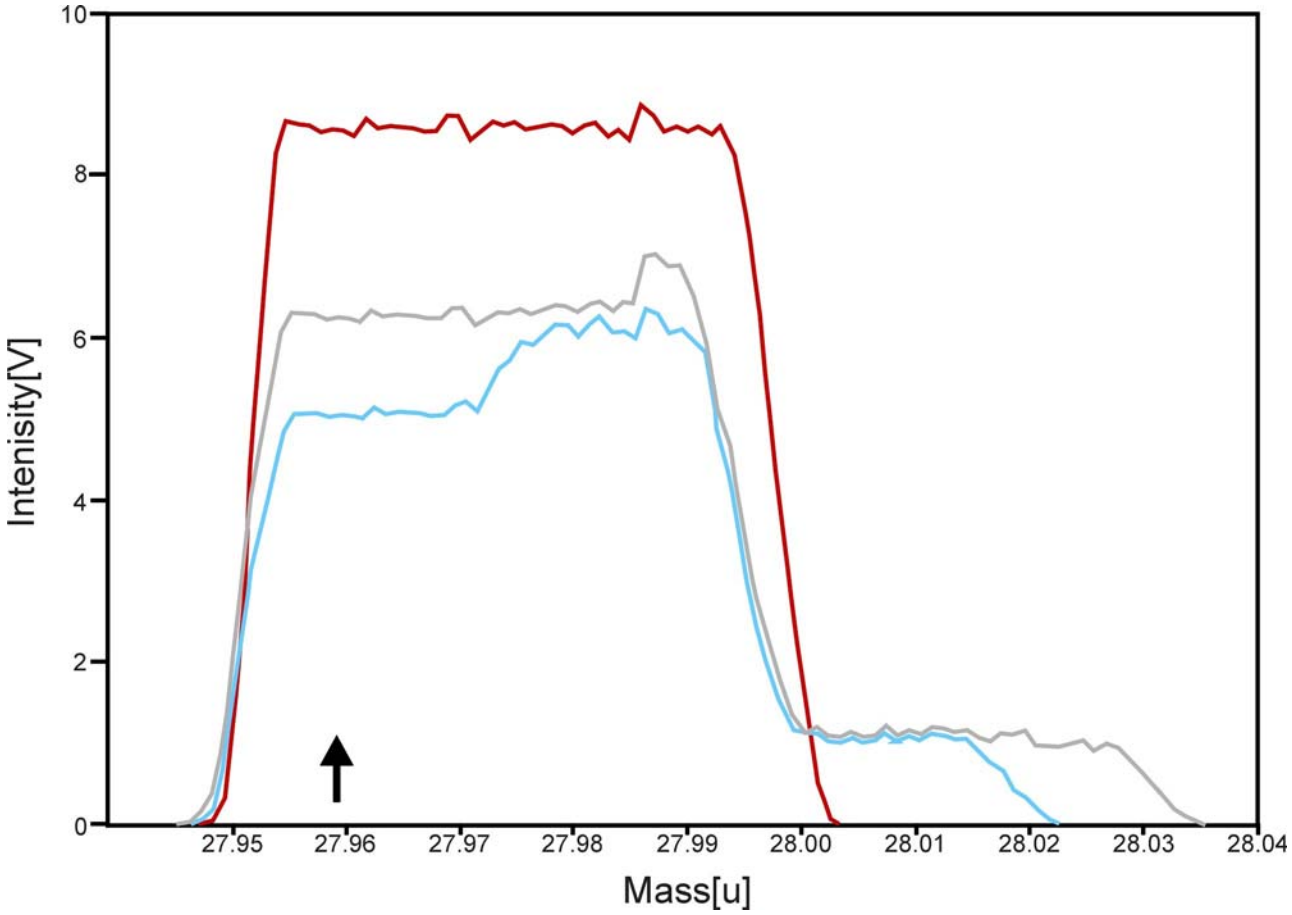
10
8
6
4
2
0
Intenisity[V]
27.95
27.96
27.97
27.98
27.99
28.00
28.01
28.02
28.03
28.04
Mass[u]

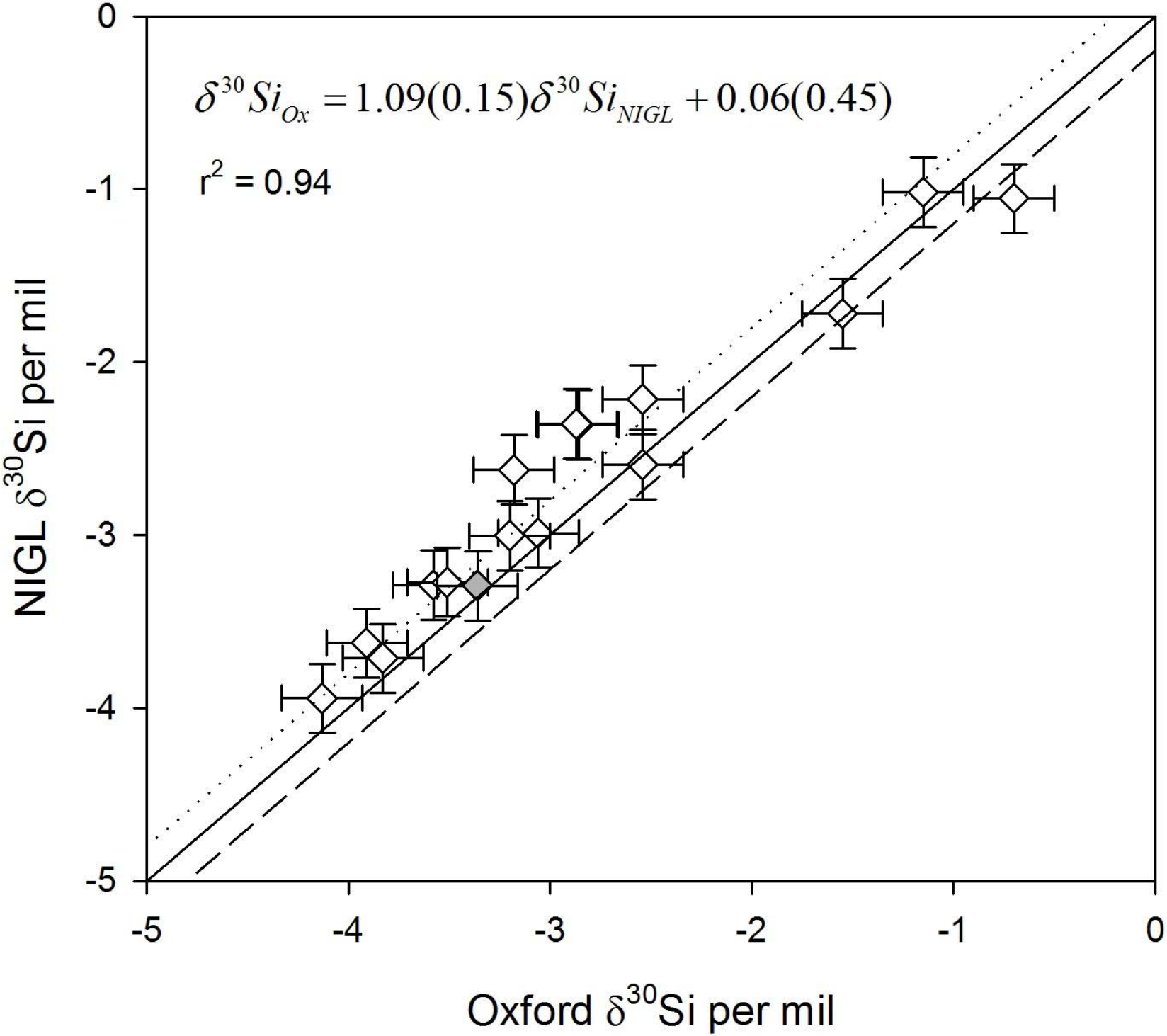
$\delta^{30}Si_{Ox} = 1.09(0.15)\delta^{30}Si_{NIGL} + 0.06(0.45)$
r² = 0.94
NIGL δ³⁰Si per mil
Oxford δ³⁰Si per mil
0
-1
-2
-3
-4
-5
-5
-4
-3
-2
-1
0

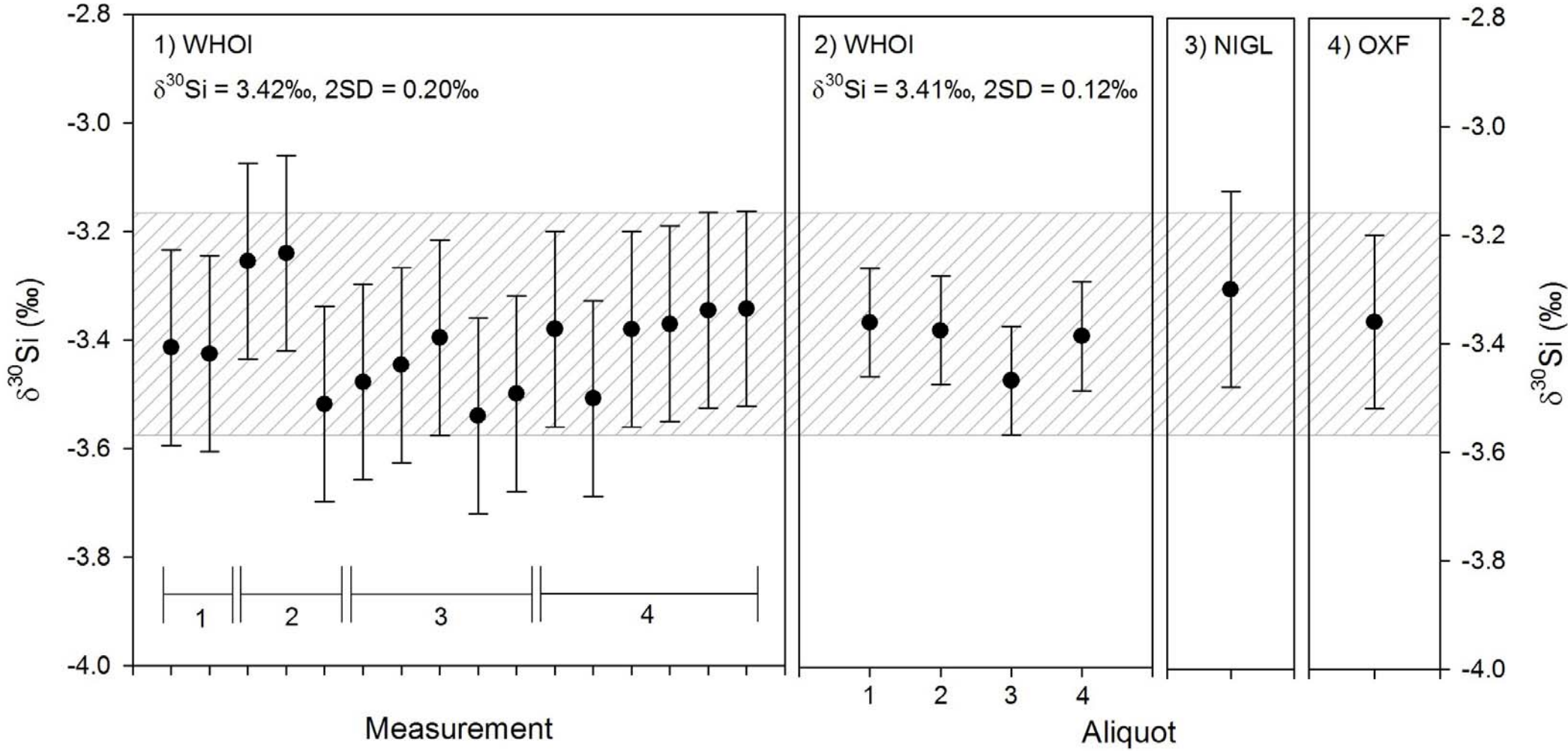
1) WHOI
δ30Si = 3.42‰, 2SD = 0.20‰
2) WHOI
δ30Si = 3.41‰, 2SD = 0.12‰
3) NIGL
4) OXF
-2.8
-3.0
-3.2
-3.4
-3.6
-3.8
-4.0
δ30Si (‰)
1
2
3
4
Measurement
Aliquot

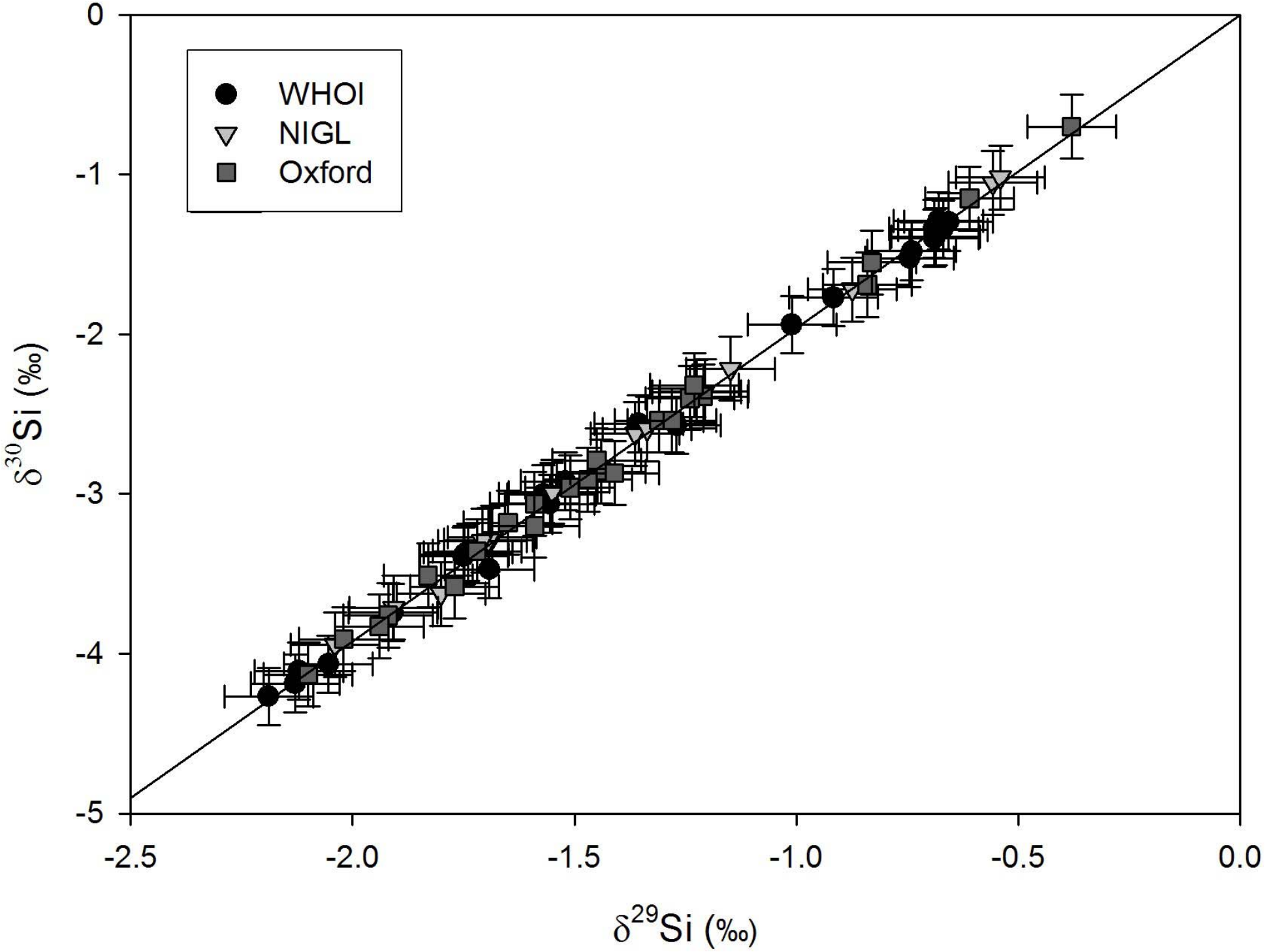
WHOI
NIGL
Oxford
0
-1
-2
-3
-4
-5
-2.5
-2.0
-1.5
-1.0
-0.5
0.0
δ30Si (‰)
δ29Si (‰)

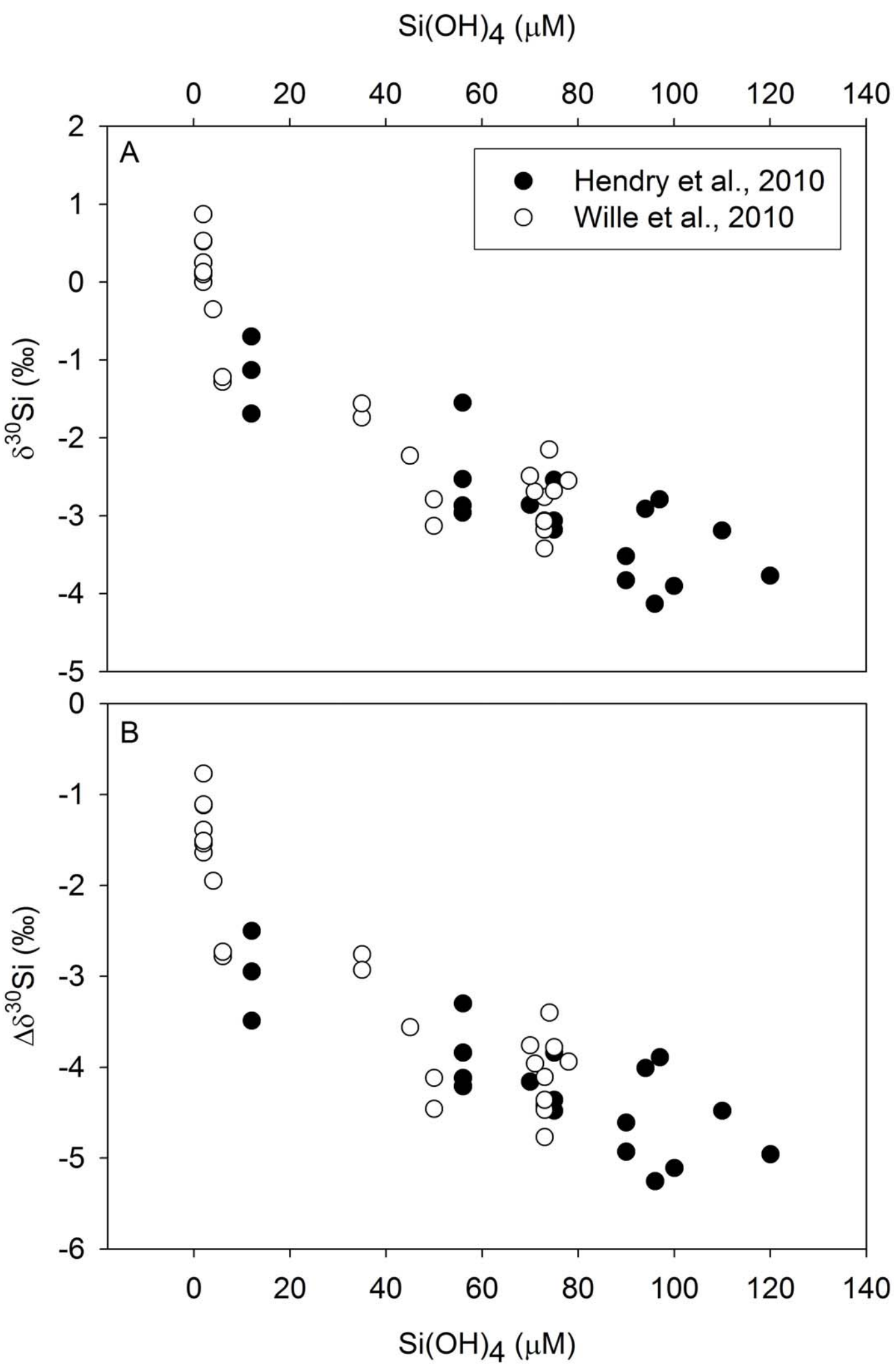
Si(OH)4 (μM)
0
20
40
60
80
100
120
140
A
Hendry et al., 2010
Wille et al., 2010
δ30Si (‰)
2
1
0
-1
-2
-3
-4
-5
B
Δδ30Si (‰)
0
-1
-2
-3
-4
-5
-6
Si(OH)4 (μM)